

**EXPERIMENTALLY VERIFIED ROBUSTNESS  
PROPERTIES OF A CLASS OF MODEL  
INVERSE ILC ALGORITHMS**

**J. J. Hätönen\* D. H. Owens <sup>\*,1</sup> J. D. Ratcliffe\*\*  
P. L. Lewin\*\* E. Rogers\*\***

*\* Department of Automatic Control and Systems  
Engineering, University of Sheffield, Sheffield, S1 3JD, UK*

*\*\* School of Electronics and Computer Science, University  
of Southampton, Southampton, SO17 1BJ, UK*

Abstract: In this paper, the subject is the robustness and noise rejection properties of an inverse type iterative learning control algorithm. As a new result it is shown that by adapting the learning gain as a function of trial number it is possible to produce a more accurate limiting error even when the plant is subject to measurement noise. This result is experimentally verified on an industrial-scale gantry robot system.

Keywords: iterative learning, inverse model, experimental verification

## 1. INTRODUCTION

Iterative Learning Control (ILC) is a relatively new addition to the toolbox of control algorithms. ILC is concerned with the performance of systems that operate in a repetitive manner. Such systems include robot arm manipulators and chemical batch processes, where the task of following some specified output trajectory  $r(t)$  in an interval  $t \in [0, N]$  with high precision is repeated time and time again. The use of conventional control algorithms with such systems will result in the same level of tracking error being repeated time and time again. Motivated by human learning, the basic idea of ILC is to use information from previous executions of the task in order to improve performance from trial to trial in the sense that the tracking error is sequentially reduced from trial-to-trial. For further background on ILC see, as two representatives of the very large literature (Arimoto *et al.*, 1984) and/or (Moore, 1993).

The concept of inverting plant dynamics to achieve perfect tracking is a simple and obvious one. However, it is hesitantly used in high precision tasks as uncertainty in plant models can lead to sub-optimal tracking and potential stability issues. Inverse models also tend to amplify measurement noise, which makes them even less attractive in feedback control applications.

This paper produces new results on how inverse models can be effectively used in the context of ILC. In particular, the robustness and noise rejection properties of an inverse model algorithm are studied in both analysis and experiment. The experimental work is based on a gantry robot system and it is important to note that this is by no means the first application of ILC see, for example, (Norrlöf, 2002) — in fact the robot system here is used to (begin the) experimental bench marking of one algorithm and, in essence, this is where the focus of this paper lies.

---

<sup>1</sup> E-mail: D.H.Owens@sheffield.ac.uk

## 2. PROBLEM DEFINITION

As a starting point consider the following standard linear, time-invariant single input, single output state-space representation defined over *finite* time interval,  $t \in [0, N]$  (in order to shorten notation it is assumed that sampling time is unity):

$$\begin{aligned} x(t+1) &= Ax(t) + Bu(t), & x(0) &= x_0 \\ y(t) &= Cx(t) \end{aligned} \quad (1)$$

where the state  $x(\cdot) \in \mathbb{R}^n$ , output  $y(\cdot) \in \mathbb{R}$ , input  $u(\cdot) \in \mathbb{R}$  and  $x(0) = 0$ . The operators  $A, B$  and  $C$  are matrices of appropriate dimensions. From now on it will be assumed that  $CB > 0$  and that the system (1) is controllable and observable. Furthermore, a reference signal  $r(t)$  is specified and the control objective is to find an input function  $u(t)$  so that the output function  $y(t)$  tracks the reference signal  $r(t)$  as accurately as possible.

This repetitive nature of the problem opens up possibilities for modifying iteratively the input function  $u(t)$  so that as the number of repetitions increases, the system learns the input function that gives perfect tracking. In particular, the basic novel feature is to construct a control law

$$u_{k+1} = f(u_k, u_{k-1}, \dots, u_{k-r}, e_{k+1}, e_k, \dots, e_{k-s}) \quad (2)$$

so that

$$\lim_{k \rightarrow \infty} \|e_k\| = 0 \quad \lim_{k \rightarrow \infty} \|u_k - u^*\| = 0 \quad (3)$$

where  $u_k = [u_k(0) \ u_k(1) \ \dots \ u_k(N)]^T$ ,  $y_k = [y_k(0) \ y_k(1) \ \dots \ y_k(N)]^T$ ,  $e_k = [r(0) - y_k(0) \ r(1) - y_k(1) \ \dots \ r(N) - y_k(N)]^T$ , and  $\|\cdot\|$  is a suitable norm. Note that if the mapping  $f$  in (2) is not a function of  $e_{k+1}$ , then it is typically said that the algorithm is of feedforward type, otherwise it is of feedback type.

For analysis purposes, note that because the system (1) is defined over a finite time-interval, it can be represented equivalently with a matrix equation  $y_k = G_e u_k$ , where

$$G_e = \begin{bmatrix} 0 & 0 & 0 & \dots & 0 \\ CB & 0 & 0 & \dots & 0 \\ CAB & CB & 0 & \dots & 0 \\ \vdots & \vdots & \vdots & \ddots & \vdots \\ CA^{N-1}B & CA^{N-2}B & \dots & \dots & 0 \end{bmatrix} \quad (4)$$

where the elements  $CA^j B$  of the matrix  $G_e$  are the Markov parameters of the plant (1). It is assumed here that the reference signal  $r(t)$  satisfies  $r(0) = Cx_0$ . Then it can be shown (see [3]) that for analysis it is sufficient to consider a “lifted” plant equation  $y_{k,l} = G_{e,l} u_{k,l}$  where  $u_{k,l} = [u_k(0) \ u_k(1) \ \dots \ u_k(N-1)]^T$ ,  $y_{k,l} = [y_k(1) \ y_k(2) \ \dots \ y_k(N)]^T$  and

$$G_{e,l} = \begin{bmatrix} CB & 0 & 0 & \dots & 0 \\ CAB & CB & 0 & \dots & 0 \\ CA^2B & CAB & CB & \dots & 0 \\ \vdots & \vdots & \vdots & \ddots & \vdots \\ CA^{N-1}B & CA^{N-2}B & \dots & \dots & CB \end{bmatrix} \quad (5)$$

Note that because it was assumed that  $CB \neq 0$ ,  $G_{e,l}$  is invertible, and consequently for an arbitrary reference  $r$  there exists  $u^*$  so that  $r = G_{e,l}u^*$ . Hence it would appear that this inverse model algorithm can be regarded as theoretically “perfect”. This, however, would require an exact system model to be available and implemented which is not a practically justified assumption — the best is that a nominal model is available or chosen deliberately to reduce the computational burden. Here this ‘lifted’ plant will be used as a starting point for analysis, and in order to shorten notation, the subscript  $l$  will be omitted.

## 3. THE INVERSE MODEL ALGORITHM

There are many possible inverse plant ILC algorithms and here as a representative we consider the case when

$$u_{k+1} = u_k + G_e^{-1} e_k \quad (6)$$

Simple analysis of the corresponding error evolution equation shows the expected result that error converges to zero in one iteration which is the perfect “solution”. This requires the “perfect” model  $G_e$  and in practice it has to be replaced by a nominal model denoted here by  $G_o$ , i.e.

$$u_{k+1} = u_k + G_o^{-1} e_k \quad (7)$$

This yields the following error evolution equation:

$$e_{k+1} = (I - G_e G_o^{-1}) e_k \quad (8)$$

The convergence characteristics of (8) depend upon the matrix  $G_e G_o^{-1}$ , a matrix which has no guarantee of stability. A simple attempt to introduce stability is to insert a scalar gain,  $\beta$ , into the algorithm.

$$u_{k+1} = u_k + \beta G_o^{-1} e_k \quad (9)$$

and hence

$$e_{k+1} = (I - \beta G_e G_o^{-1}) e_k \quad (10)$$

A necessary and sufficient condition for stability is for the spectral radius of  $(I - \beta G_e G_o^{-1})$  to be less than 1 but satisfying this may still lead to very poor performance of the algorithm. This paper allows  $\beta$  to vary in such a manner that the  $l_2$ -norm of the error is monotonically decreasing which is obviously a very useful property of an ILC algorithm. More precisely, the update equation and the error dynamics are determined by

$$u_{k+1} = u_k + \beta_{k+1} G_o^{-1} e_k \quad (11)$$

$$e_{k+1} = (I - \beta_{k+1}G_eG_o^{-1})e_k \quad (12)$$

Norm Optimal Iterative Learning Control (NOILC) (Amann *et al.*, 1995) is one Optimal ILC routine that has been shown to give monotonic error convergence in spite of some model uncertainties. NOILC minimizes both the error and the change in input between trials by computing  $\min_{u_{k+1} \in \mathbb{R}^N} J(u_{k+1})$  where the cost function  $J(u_{k+1})$  is given (Arimoto *et al.*, 1984) by

$$J(u_{k+1}) = \|e_{k+1}\|^2 + \|u_{k+1} - u_k\|^2 \quad (13)$$

where the  $l_2$ -norm is used. This framework extends to the use of the adaptive update law (11) by using

$$J(\beta_{k+1}) = \|e_{k+1}\|^2 + w\beta_{k+1}^2 \quad (14)$$

where  $w$  can be freely chosen such that  $w > 0$ . This cost function adds flexibility whilst still maintaining the NOILC ideal of minimizing error and smoothing changes in input. For the case  $G_o = G_e$  a straightforward minimization of (14) yields an optimal solution:

$$\beta_{k+1} = \frac{\|e_k\|^2}{w + \|e_k\|^2} \quad (15)$$

A convergence analysis of this algorithm for the case  $G_o = G_e$  is given next.

*Proposition 1.* If  $G_o = G_e$ ,  $w \in \mathbb{R}$ ,  $w > 0$  then  $\|e_{k+1}\| < \|e_k\|$  if  $e_k \neq 0$ . Furthermore,

$$\lim_{k \rightarrow \infty} \|e_k\| = 0 \text{ and } \lim_{k \rightarrow \infty} \beta_{k+1} = 0 \quad (16)$$

demonstrating monotonic convergence to zero tracking error.

**Proof.** Selecting a sub-optimal choice  $\beta_{k+1} = 0$  in the cost function (14) yields  $J(0) = \|e_k\|^2$ . Since this choice is sub-optimal it follows:

$$\|e_k\|^2 \geq \|e_{k+1}\|^2 + w\beta_{k+1}^2 \geq \|e_{k+1}\|^2 \quad (17)$$

demonstrating monotonic convergence. Reformulation of (17) gives

$$\|e_k\|^2 - w\beta_{k+1}^2 \geq \|e_{k+1}\|^2 \geq 0 \quad (18)$$

and applying induction further gives

$$\|e_0\|^2 - w \sum_{i=1}^{k+1} \beta_i^2 \geq 0 \quad (19)$$

and because  $k$  is arbitrary,  $\lim_{k \rightarrow \infty} \beta_k = 0$ . This results in

$$0 = \lim_{k \rightarrow \infty} \beta_{k+1} = \lim_{k \rightarrow \infty} \frac{\|e_k\|^2}{w + \|e_k\|^2} \quad (20)$$

This is only possible if  $\lim_{k \rightarrow \infty} e_k = 0$ . Furthermore, the interlacing result (17) implies that  $\|e_{k+1}\| < \|e_k\|$  if  $e_k \neq 0$  which completes the proof of Proposition 1.  $\square$

*Remark 1.* The choice of  $w = w_1\|e_k\|^2$  in (15) where  $G_o = G_e$  yields the error evolution equation  $e_{k+1} = (1 - (1 + w_1)^{-1})e_k$ . Then for any  $w_1 > 0$  error convergence is geometric.

#### 4. ROBUSTNESS OF THE INVERSE MODEL ALGORITHM

Robustness of ILC algorithms is an active research topic and space limitations preclude a summary of the many approaches and their relative limitations/merits. Here we undertake an analysis of the algorithm of the previous section both in terms of system stability and performance by retaining monotonic convergence in the presence of model uncertainty. For this we need an uncertainty representation and here we consider the case when the true plant,  $G_e \neq G_o$ , and the model uncertainty of  $G_o$  is taken to be a multiplicative matrix  $U$ , i.e.  $G_e = G_oU$ . The first result is as follows.

*Proposition 2.* Suppose  $U + U^T$  is a positive-definite matrix. If  $e_k \neq 0$  there exists a  $\beta_{k+1} > 0$  such that  $\|e_{k+1}\|^2 - \|e_k\|^2 < 0$ . Furthermore the value of such  $\beta_{k+1}$  has to satisfy the following inequality

$$v^T \left( \frac{1}{\beta_{k+1}} I - U \right)^T \left( \frac{1}{\beta_{k+1}} I - U \right) v < \frac{1}{\beta_{k+1}^2} \|v\|^2 \quad (21)$$

where  $v \in \mathbb{R}^N$  is arbitrary.

*Proof 1.* Use of (9) yields

$$\|e_{k+1}\|^2 - \|e_k\|^2 = -2\beta_{k+1}e_k^T U e_k + \beta_{k+1}^2 e_k^T U^T U e_k < 0 \quad (22)$$

Since  $U + U^T$  is assumed to be a positive-definite matrix and  $\beta_{k+1} > 0$ , the terms  $-2\beta_{k+1}e_k^T U e_k$  and  $\beta_{k+1}^2 e_k^T U^T U e_k$  are, for an arbitrary nonzero  $e_k$ , strictly positive and strictly negative respectively. Then for  $\|e_{k+1}\|^2 < \|e_k\|^2$  it is necessary that the following inequality must be true.

$$2\beta_{k+1}e_k^T U e_k > \beta_{k+1}^2 e_k^T U^T U e_k \quad (23)$$

Since the left hand term of inequality (23) is of  $O(\beta_{k+1})$  and the right hand term is of  $O(\beta_{k+1}^2)$  it shows that the inequality is met for a sufficiently small  $\beta_{k+1}$ , giving monotonic convergence. Completing the square in (23) now gives (21).

Proposition 2 shows that if (21) holds true then error convergence is monotonic. The next proposition further shows that under this condition the error converges to zero. The proof of this result follows from that of Proposition 2 and hence the details are omitted here.

*Proposition 3.* If the condition in Proposition 2 holds then  $\lim_{k \rightarrow \infty} e_k = 0$ .

*Remark 2.* Note that it is easy to show that a sufficient condition for  $U + U^T$  to be a positive-definite system is that the underlying system  $U(z)$  corresponding to  $U$  is a positive-real system. The phase shift of such a system lies within  $\pm 90^\circ$  for all

frequencies. Therefore the algorithm can tolerate a plant uncertainty of  $\pm 90^\circ$  phase shift for all frequencies.

The next proposition shows how the use of the adaptive  $\beta_{k+1}$  given in (15) can ensure that (21) holds by taking  $w$  to be a sufficiently large positive number.

*Proposition 4.* Assume  $U + U^T$  is positive-definite and  $w$  is sufficiently large. In this case a sufficient condition for monotonic convergence is that

$$w > \|e_0\|^2 \left( \frac{\sigma_{\max}(U^T U)}{\sigma_{\min}(U + U^T)} - 1 \right) \quad (24)$$

where  $\sigma_{\max}(U^T U)$  is largest eigenvalue of the matrix  $U$  and  $\sigma_{\min}(U + U^T)$  is the smallest eigenvalue of the matrix  $U + U^T$ .

*Proof 2.* Substituting (15) into inequality (23) with a couple of algebraic manipulations gives a necessary and sufficient condition for monotonic convergence

$$w > \frac{\|e_k\|^2 e_k^T U^T U e_k}{2e_k^T U e_k} - \|e_k\|^2 \quad (25)$$

Making the two estimates

$$\sigma_{\max}(U^T U) \|e_k\|^2 \geq e_k^T U^T U e_k \quad (26)$$

and

$$\sigma_{\min}(U + U^T) \|e_k\|^2 \leq 2e_k^T U e_k \quad (27)$$

a the sufficient condition for convergence becomes

$$w > \|e_k\|^2 \left( \frac{\sigma_{\max}(U^T U)}{\sigma_{\min}(U + U^T)} - 1 \right) \quad (28)$$

Since the initial guess  $u_0$  results in a bounded tracking error  $e_0$  then for any  $w$  such that inequality (28) holds, i.e. a  $w$  that ensures  $\|e_0\| \geq \|e_1\|$ , then inequality (28) will also hold for  $e_k = e_1$ . Inductively condition (24) holds for an arbitrary iteration  $k$  and therefore convergence is monotonic.

*Remark 3.* Note that from (28) the sufficient value of  $w$  decreases as  $\|e_k\|$  decreases. Since an excessively large  $w$  will give a small  $\beta_{k+1}$  implying  $u_{k+1} \approx u_k$  then decreasing  $w$  with each iteration will result in faster convergence. An obvious method to exploit this without violating (28) is to set  $w = w_1 \|e_k\|^2$  where  $w_1$  is both sufficiently large and constant from iteration to iteration.

As noted in the previous section, for the nominal case  $G_e = G_o$  the selection of  $w = w_1 \|e_k\|^2$  in fact gives geometric error convergence. The next proposition extends this to the case where  $G_e$  has positive multiplicative uncertainty.

*Proposition 5.* If  $U + U^T$  is a positive-definite matrix and  $e_k \neq 0$  then there exists a  $w$  such that  $\|e_{k+1}\| \leq \alpha \|e_k\|$  where  $0 \leq \alpha < 1$ .

*Proof 3.* The choice of  $w = w_1 \|e_k\|^2$  yields the following equation for  $\|e_{k+1}\|^2$

$$\|e_{k+1}\|^2 = \|e_k\|^2 - \gamma 2e_k^T U e_k + \gamma^2 e_k^T U^T U e_k \quad (29)$$

where  $\gamma = (1 + w_1)^{-1}$ . Note that since  $U + U^T$  is positive-definite then the second and third right-hand terms in (29) are strictly negative and strictly positive respectively for an arbitrary  $e_k \neq 0$ . Using the estimates in (26) and (27) gives

$$\|e_{k+1}\|^2 \leq \alpha^2 \|e_k\|^2 \quad (30)$$

where

$$\alpha^2 = 1 - \gamma \sigma_{\min}(U + U^T) + \gamma^2 \sigma_{\max}(U^T U) \quad (31)$$

Since the negative term  $-\gamma \sigma_{\min}(U + U^T)$  is of  $O(1 + w_1)^{-1}$  and the positive term  $\gamma^2 \sigma_{\max}(U^T U)$  is of  $O(1 + w_1)^{-2}$  then by using a sufficiently large  $w_1 > 0$  it is ensured that  $0 \leq \alpha < 1$ , giving geometric convergence.

*Remark 4.* Note that if  $\beta_{k+1}$  is chosen to be as in (15) then  $\beta_{k+1}$  will decrease with  $\|e_k\|$  allowing for a greater degree of positive uncertainty in  $G_e$  to be tolerated. Therefore the better the initial guess for input  $u_0$ , the smaller  $\|e_0\|$  becomes and the more positive uncertainty the controller can tolerate.

*Remark 5.* Choosing a very large  $w$  during the early trials gives  $\beta_{k+1} \simeq 0$ . Clearly this choice increases the robustness margin but at the same time decreases convergence speed.

## 5. MEASUREMENT NOISE ANALYSIS

This section analyzes the effect of measurement noise upon the performance of an inverse type ILC algorithm. Random measurement noise obviously prevents the error from reaching zero, although reduction in error can be obtained when the error to signal to noise ratio is high. The analysis in this section shows that by decreasing a fixed learning gain  $\beta$ , the limiting error of the system can be expected to decrease. In order to initiate the analysis, consider the control law

$$u_{k+1} = u_k + \beta G_o^{-1} (r - y_k - n_k) \quad (32)$$

where  $1 > \beta > 0$ , and the noise free tracking error

$$e_{k+1} = r - G_o u_{k+1} \quad (33)$$

where  $n_k$  models the effect of measurement noise. From now on it is assumed that the measurement noise is zero-mean Gaussian white noise, and satisfies the equation

$$E(n_j^T n_{k+1}) = \begin{cases} \mu^2, j = k + 1 \\ 0, j \neq k + 1 \end{cases} \quad (34)$$

*Proposition 6.* Under the assumptions of perfect plant model and Gaussian white (measurement) noise the inverse algorithm satisfies

$$\lim_{k \rightarrow \infty} E(e_{k+1}^T e_{k+1}) = \frac{\beta \mu^2}{2 - \beta} \quad (35)$$

for an arbitrary initial condition  $e_0$ .

**Proof.** Straightforward manipulations show that the inverse algorithm (32) results in the following error evolution equation under the presence of measurement noise:

$$e_{k+1} = (1 - \beta)e_k + \beta n_k \quad (36)$$

Taking the inner product between (36) and  $e_{k+1}$  shows that the error evolution equation in terms of squared norms is given by

$$\|e_{k+1}\|^2 = (1 - \beta)^2 \|e_k\|^2 + 2(1 - \beta)\beta e_k^T n_k + \beta^2 \|n_k\|^2 \quad (37)$$

Finally, because  $n_k$  satisfies (34) and  $e_k = r - G_e u_k$  is a deterministic signal, taking the expected value of  $\|e_{k+1}\|^2$  in (37) shows that equation (37) can be simplified to

$$E(\|e_{k+1}\|^2) = (1 - \beta)^2 E(\|e_k\|^2) + \beta^2 \mu^2 \quad (38)$$

It follows then that as the iteration  $k$  approaches *infinity* the limiting error becomes

$$\begin{aligned} \lim_{k \rightarrow \infty} E(e_{k+1}^T e_{k+1}) &= \lim_{k \rightarrow \infty} (1 - \beta)^{2k} E(e_0^T e_0) \\ &+ \sum_{i=0}^{\infty} ((1 - \beta)^2)^i \beta^2 \mu^2 \\ &= \frac{\beta^2 \mu^2}{1 - (1 - \beta)^2} = \frac{\beta \mu^2}{2 - \beta} \end{aligned}$$

which completes the proof.  $\square$

*Remark 6.* Note that the value of the expectation of the limiting  $l_2$  error is independent of  $e_0$  since the control scheme has still iteratively learned to reject this initial error. The result clearly shows that as  $\beta$  approaches zero the expected error converges to zero. Of course as  $\beta$  tends to zero, so does convergence speed and this result highlights a second trade-off for inverse-type ILC: convergence speed versus limiting error in the face of unknown measurement noise.

In practical applications, however, the model is never exactly known. Therefore the next proposition characterizes the expected value of the norm of the limiting error under the presence of multiplicative uncertainty  $U$ , i.e.  $y_{k+1} = G_e u_{k+1} = U G_o u_{k+1}$  and  $u_{k+1} = u_k + \beta G_o^{-1}(e_k - n_k)$ .

*Proposition 7.* Suppose that  $U + U^T$  is a positive-definite matrix and that  $\beta$  is sufficiently small. In this case the limiting error satisfies the bound

$$\sup_{k \rightarrow \infty} E(\|e_{k+1}\|^2) \leq \frac{\beta m_2^2 \mu^2}{m_1^2 - \beta m_2^2} \quad (39)$$

where  $m_1^2$  is the smallest eigenvalue of  $U + U^T$  and  $m_2^2$  is the largest eigenvalue of  $U^T U$ .

*Proof 4.* Straightforward manipulations show that the error evolution equation in the case of multiplicative uncertainty is given by

$$e_{k+1} = (I - \beta U)e_k + \beta U n_k \quad (40)$$

and therefore

$$\|e_{k+1}\|^2 = e_k^T (I - \beta U)^T (I - \beta U) e_k + 2e_k^T \beta (I - \beta U)^T U n_k + \beta^2 n_k^T U^T U n_k \quad (41)$$

Taking the expected value on this result shows that

$$E(\|e_{k+1}\|^2) \leq (1 - \beta m_1^2 + \beta^2 m_2^2) E(\|e_k\|^2) + \beta^2 m_2^2 E(\|n_k\|^2) \quad (42)$$

where  $m_1^2$  is the smallest eigenvalue of  $U + U^T$  and  $m_2^2$  is the largest eigenvalue of  $U^T U$ . Taking  $\beta$  sufficiently small guarantees that  $(1 - \beta m_1^2 + \beta^2 m_2^2) < 1$  and using a similar argument as in the proof above shows that

$$\begin{aligned} \sup_{k \rightarrow \infty} E(\|e_{k+1}\|^2) &\leq \frac{\beta^2 m_2^2 \mu^2}{1 - (1 - \beta m_1^2 + \beta^2 m_2^2)} \\ &= \frac{m_2^2 \mu^2 \beta}{m_1^2 - \beta m_2^2} \end{aligned} \quad (43)$$

which concludes the proof.

*Remark 7.* Even though this proposition is potentially conservative, it still shows that by reducing  $\beta$  it is possible to reduce the expectation of the limiting error. This will initially lead to slower convergence, demonstrating again the trade-off between convergence speed and limiting accuracy. The analysis also demonstrates that if  $m_2^2$  (the largest eigenvalue of  $U^T U$ ) is very large (for example  $U(z)$  has a resonance), it will have a negative effect on the limiting performance. Thus with resonant systems, problems with measurement noise are more likely to occur than with non-resonant systems.

*Remark 8.* Note the analysis in this section holds only for a constant learning gain  $\beta$ . The adaptive algorithm, however, automatically reduces  $\beta$  as function of the iteration index  $k$ , and therefore it is anticipated that the adaptive algorithm can ‘automatically’ produce a good balance between convergence speed and asymptotic accuracy. Any theoretical results in this direction will be reported separately.

## 6. EXPERIMENTAL RESULTS

A multi-axis test facility has been constructed so as to practically test ILC on a wide range of dynamic systems in an industrial-style application.

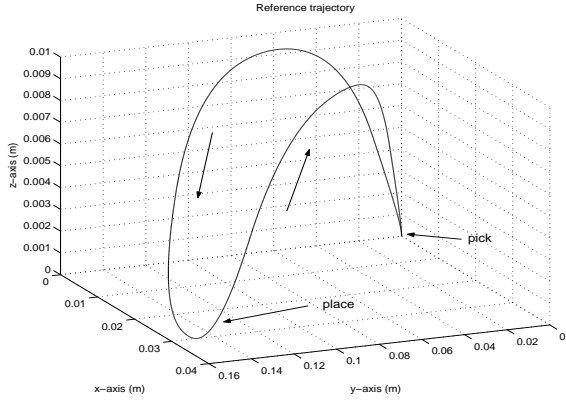


Fig. 1. 3D reference trajectories

Currently, the apparatus consists of a three-axis gantry robot supported above one end of a 6m long industrial plastic chain conveyor. A description of the test facility can be found in (Ratcliffe *et al.*, 2004b). A 100Hz sample frequency was used to calculate the inverse models for each axis. The combined displacement reference trajectories for each axis (Figure 1) produce a ‘pick and place’ action, designed to collect a payload from a dispenser, synchronise position and velocity with the conveyor and place the payload on the conveyor. The reference trajectories define the iteration time period as 2 seconds. With a 100Hz sample frequency, this results in 200 sample instants per iteration.

The inverse algorithm has been implemented with a range of values for  $\beta$ , in order to experimentally verify the algorithms performance. Space limitations preclude a comprehensive discussion of the results but the effect of  $\beta$  on limiting performance in the presence of measurement noise is included as an illustration. This has been investigated by deliberately adding bounded, zero-mean, pseudo-random noise to the axis displacement signal recorded from the test facility by optical incremental encoders. The noise is pseudo-random, because it is generated by a seeded random number generator. In these experiments, the seed is the product of the sample number and the iteration number. Therefore for different iterations, the added noise appears to be random. However, for different tests, the same value of noise is added for corresponding samples during corresponding iterations.

Figure 2 displays the mean squared tracking error (mse) on a logarithmic scale (in  $\text{mm}^2$ ) recorded for each iteration, with learning gain  $\beta$  equal to 0.1, 0.2 and 0.3. The pseudo-random noise has maximum bounds specified as  $\pm 0.1\text{mm}$ . Similar results were obtained for the Y and Z axes and hence the plots have been omitted here. Previous experimental work has shown that the inverse algorithm is sensitive to the combination of measurement noise and high-frequency non-linearities.

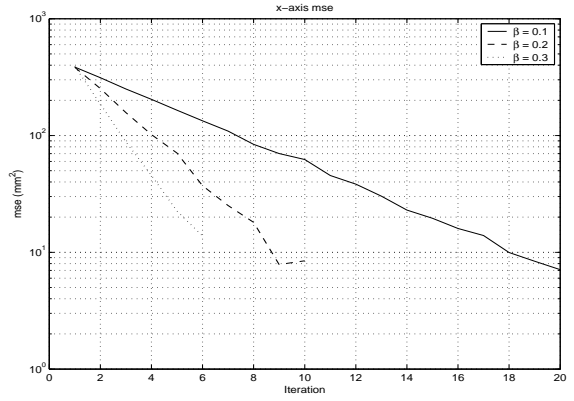


Fig. 2. X-axis mse with  $\beta = 0.1, 0.2$  and  $0.3$  ( $\pm 0.1\text{mm}$  bounded noise)

The noise builds up in the iteration loop due to high-frequency nonlinearities, rapidly corrupting the plant input signal and causing much degraded performance.

The figures clearly demonstrate that convergence speed is proportional to  $\beta$  whereas minimum mse attained is inversely proportional to  $\beta$ , i.e. a trade-off is evident. This analysis is somewhat biased by how many iterations the algorithm can perform before the noise becomes sufficiently large to force a system shutdown. Therefore it is necessary to develop a test where the control system converges to minimum error and remains stable.

Zero-phase filtering has been shown to successfully stabilize the inverse ILC algorithm considered here in practical experiments (Ratcliffe *et al.*, 2004a). A discrete low-pass, 3rd order Chebychev filter, designed for a 100Hz sample frequency and producing 20dB of attenuation at 15Hz is implemented on the ILC generated plant input, before the vector is supplied to the robot. The filter transfer function is represented by:

$$\frac{y(z)}{u(z)} = \frac{0.102693 + 0.002934z^{-1}}{1 - 1.644597z^{-1}} \cdots + \frac{0.002934z^{-2} + 0.102693z^{-3}}{+1.091881z^{-2} - 0.236029z^{-3}} \quad (44)$$

Figure 3 displays the X axis mse plots for  $\beta$  equal to 0.2 and 0.8, when the added noise lies within the bounds  $\pm 1\text{mm}$ . (The corresponding plots for the Y and Z axes are similar and hence omitted here.) A larger error bound can be tolerated because the low pass filter inherently attenuates signals above the cut-off frequency. Larger error must be added if a component of the noise is to pass through the filter to interfere with the learning algorithm. The inverse algorithm stability has been improved and the mse now reaches minimum tracking error and maintains this level of error consistently. Clearly, for the X axis the larger gain of 0.8 produces a larger residual tracking error

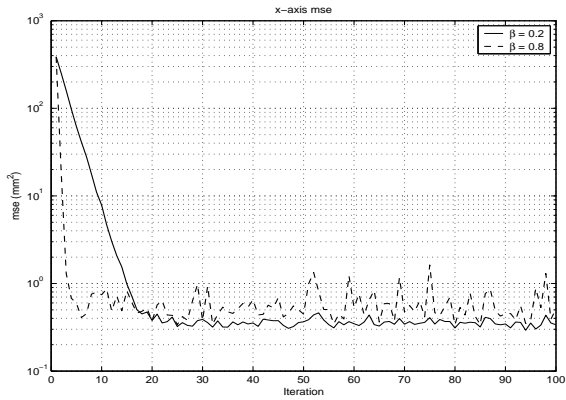


Fig. 3. X-axis mse with  $\beta = 0.2$  and  $0.8$  ( $\pm 1$ mm bounded noise, including zero-phase filter)

in the limit than the smaller gain of 0.2. But, the larger gain still produces initial faster convergence. For detailed experimental results on the effect of modelling uncertainty on the algorithm performance.

## 7. CONCLUSIONS

The use of inverse type ILC in the past has been unpopular owing to the belief that it lacks robustness. This paper however, shows that if an adaptive learning gain is added to the algorithm the system will geometrically converge if the plant multiplicative uncertainty satisfies a positivity condition. The adaptive learning gain is selected by the optimization of an objective function that balances the reduction of the tracking error with the size of the learning gain. As a new theoretical result it has been shown that by decreasing the learning gain it is possible to achieve satisfactory tracking accuracy under the presence of measurement noise. This new result has been validated on an industrial-scale gantry robot system. Future work will include an investigation into the effects of measurement noise on the performance of the adaptive inverse algorithm. Furthermore, design rules for selecting the free parameters of the adaptive cost function are sought as a function of the measurement noise variance.

The results here only deal with one class of inverse ILC algorithms. In other work, see, for example, (Saab, 2001; Saab, 2003) ILC algorithms (P-type or D-type) similar to the one considered here are analyzed where the learning gain is also tuned to decrease from iteration-to-iteration in the presence of plant uncertainty, disturbance and measurement noise. This work also extends to more general classes of plant models but no results have yet been reported on its experimental performance. This area is also one to which profitable future research should be directed.

## REFERENCES

- Amann, N., D.H. Owens and E. Rogers (1995). Iterative learning control for discrete time systems using optimal feedback and feedforward actions. In: *Proceedings of the 34th Conference on Decision and Control, New Orleans, LA*. pp. 1696–1701.
- Arimoto, S., S. Kawamura and F. Miyazaki (1984). Bettering operation of robots by learning. *Journal of Robotic Systems* **1**, 123–140.
- Moore, K. L. (1993). *Iterative Learning Control for Deterministic Systems*. Springer-Verlag.
- Norrlöf, M. (2002). An adaptive iterative learning control algorithm with experiments on an industrial robot. *IEEE Transactions on Robotics and Automation* **18**(2), 245–251.
- Ratcliffe, J.D., E. Rogers, T.J. Harte, J.J. Hätönen, P.L. Lewin and D.H. Owens (2004a). Experimental testing of a new iterative learning control algorithm. In: *Proceedings of UKACC Control 2004, Bath, UK, ID-215*.
- Ratcliffe, J.D., T.J. Harte, J.J. Hätönen, P.L. Lewin, E. Rogers and D.H. Owens (2004b). Practical implementation of a model inverse iterative learning controller. In: *Proceedings of IFAC Workshop PSYCO 04*. pp. 687–692.
- Saab, S. S. (2001). A discrete-time stochastic learning control algorithm. *IEEE Transactions on Automatic Control* **46**(6), 877–887.
- Saab, S. S. (2003). Stochastic p-type/d-type iterative learning control algorithms. *International Journal of Control* **76**(2), 139–148.